


Finite-range bias in fitting three-body loss to the zero-range model

Sofia Agafonova[✉], Mikhail Lemeshko, and Artem G. Volosniev[✉]

Institute of Science and Technology Austria (ISTA), Am Campus 1, 3400 Klosterneuburg, Austria

 (Received 14 February 2023; accepted 24 May 2023; published 20 June 2023)

We study the impact of finite-range physics on the zero-range-model analysis of three-body recombination in ultracold atoms. We find that temperature dependence of the zero-range parameters can vary from one set of measurements to another as it may be driven by the distribution of error bars in the experiment, and not by the underlying three-body physics. To study finite-temperature effects in three-body recombination beyond the zero-range physics, we introduce and examine a finite-range model based upon a hyperspherical formalism. The systematic error discussed in this Letter may provide a significant contribution to the error bars of measured three-body parameters.

DOI: [10.1103/PhysRevA.107.L061304](https://doi.org/10.1103/PhysRevA.107.L061304)

Introduction. Three-body recombination loss in cold-atom experiments provides an invaluable tool in fundamental studies of three-body physics, in particular of the Efimov effect [1–10]. Although many features of the experimental data are captured by zero-range models, current experiments also reveal finite-range effects [11–13], which require theoretical analysis of the corresponding physics.

To analyze three-body loss, one considers the number of particles lost from the system per unit of time, α . In ultracold dilute gases, α depends on a handful of quantities that characterize particle-particle interactions [6–8]. The first one is the scattering length a , which can be controlled using external fields [14]. Minimal zero-range models have two more parameters that define short-range three-body physics and the probability to recombine [6], denoted (for $a < 0$) as a_- and η . Their values are obtained from experimental data [7,8] and are often considered to be intrinsic to the few-body system at hand. However, it was observed that a_- depends on temperature [11,12], contradicting theoretical expectations. This dependence attributed to the finite-range physics (always present in realistic systems) is modeled in our Letter.

We show that the temperature dependence of a_- may be driven by the distribution of error bars in the experiment, and not by the underlying three-body physics. This is a consequence of the fact that the parameters a_- and η describe measurements only from the point of view of an incomplete (zero-range) theory—they may contain (besides intrinsic few-body physics) information about the experiment.

Our results add a possible systematic bias to the family of already known ones caused, for example, by high densities [15] or uncertainties in the trap frequencies and atom number [16]. However, unlike the previously known issues with analysis of three-body recombination, one is required to deepen *theoretical* understanding of microscopic physics to mitigate the bias discussed below. This can be important for studies of the van der Waals universality, which provides an estimate of a_- at zero temperature, $T = 0$ [17]. To test it in a laboratory, one performs a number of measurements at different temperatures and extrapolates the fitted a_- to the limit $T \rightarrow 0$ [11,12,15]. As we demonstrate, this procedure

may be inconclusive. It is an example of a much more general phenomenon—ambiguity of fits based on universal theories in the presence of nonuniversal physics. The corresponding systematic errors are not well understood in the context of cold-atom setups. Although, they should be analyzed on a case-by-case basis, some physical intuition can be adopted from other branches of physics, in particular, from studies of a few nucleons [18,19].

Illustrative toy model. Before discussing three-body recombination, let us discuss an example that provides insight into the fact that if a fitting model does not describe every relevant aspect of the data (incomplete or underfit model), then its parameters may depend on characteristics of the experiment. Moreover, the values extracted from different experiments may not overlap within respective error bars, leading to a systematic bias in the analysis. To illustrate this rather general statement, we introduce and discuss a toy model. The model is linear by design; i.e., the fitting function is a linear function of the parameters. This will allow us to gain some analytical insight into the problem.

Consider an artificial physical process described by

$$\mathcal{A}(x) = x + e^{-x^2}x, \quad (1)$$

where x is some parameter, e.g., a dimensionless length scale, and $\mathcal{A}(x)$ is an observable. Interpretation of Eq. (1) is as follows: (i) for $x \rightarrow \infty$ the system obeys the “universal” physics ($\mathcal{A} \rightarrow x$), and (ii) for $x \rightarrow 0$, some “nonuniversal” physics is important, which, for simplicity, is parametrized here by $e^{-x^2}x$.

Let us assume that there are two experiments that measure \mathcal{A} at different values of x . Each experiment produces a data set $[\{\mathcal{A}_i(x_1), \epsilon_i(x_1)\}, \{\mathcal{A}_i(x_2), \epsilon_i(x_2)\}, \dots, \{\mathcal{A}_i(x_N), \epsilon_i(x_N)\}]$. Here, the subscript denotes the experiment. ϵ_i denotes the corresponding error in the measurement of \mathcal{A} . It is assumed that the value of x is known exactly in each experiment so that there are no associated error bars. It is also assumed that both experiments measure at identical values of x . As will become clear later, these assumptions are not essential.

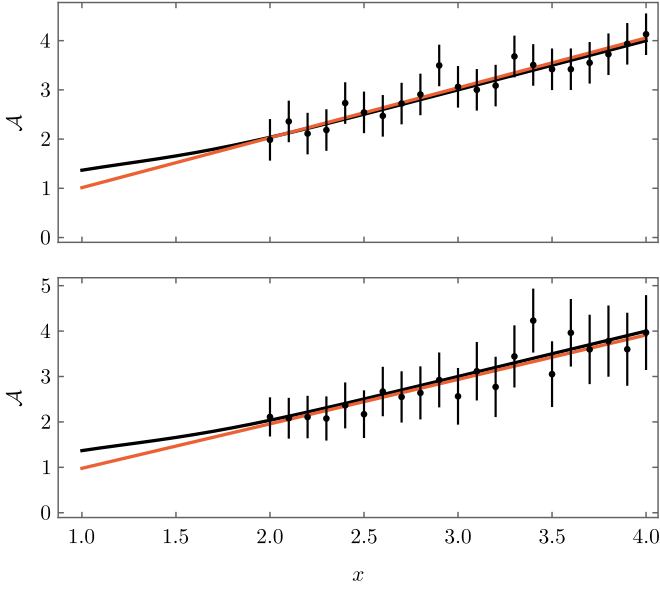


FIG. 1. Illustration of the toy model for one representative set of parameters. The black curves show the exact model of Eq. (1). The dots with error bars correspond to generated “experimental” data for $x = \{2, 2.1, 2.2, \dots, 4\}$. The data are drawn from the normal distribution with the mean given by Eq. (1) and the standard deviation by $\epsilon_i/2$. The upper panel is for $\epsilon_1 = 0.4$, and the lower panel is for $\epsilon_2 = 0.4\mathcal{A}(x)/\mathcal{A}(x_1)$. The orange curves show the best linear fit to the experimental data.

To simulate data measured in each experiment, we draw random values \mathcal{A}_i for each x from a normal distribution with the mean given by Eq. (1) and the standard deviation by $\epsilon_i/2$. The two experiments differ *only* in the values of ϵ_i . In the first experiment, we assume $\epsilon_1 = \epsilon$, and in the second one we assume $\epsilon_2(x_k) = \mathcal{A}(x_k)\epsilon/\mathcal{A}(x_1)$. Both choices appear logical—the first corresponds to a fixed error, and the second corresponds to an error proportional to the value of \mathcal{A} .

To analyze the data, we assume that the functional dependence of the universal physics is known; i.e., it is known that $\mathcal{A}_i(x_k) \simeq x_k$ in the limit $x_k \rightarrow \infty$. Therefore, we fit the data with $a_i x$, where a_i is a fit parameter [20] (see Fig. 1). It is clear that the value of a_i depends on the number of data points, N , as well as on the range of x , i.e., on x_1 and x_N . For example, if there are “sufficiently” many data points in the universal regime, i.e., with $x \gg 1$, then the mean values of a_1 and a_2 should approach 1. Here, we are interested in the scenario in which the parameter a_i contains some information about nonuniversal physics, which is a typical experimental situation. To take this into account, we fix $x_1 = 2$ and $x_N = 4$. This region is “almost” universal, as $e^{-x^2} \sim 0.018$; however, it still contains some information about the small- x region.

To determine a_i , we minimize χ^2 (“chi squared”) [21,22]:

$$\chi_i^2 = \sum_{k=1}^N \left(\frac{\mathcal{A}_i(x_k) - a_i x_k}{\epsilon_i(x_k)} \right)^2. \quad (2)$$

After differentiating χ_i^2 with respect to a_i , we derive

$$a_i = \frac{\sum_k [\mathcal{A}_i(x_k) x_k / \epsilon_i(x_k)^2]}{\sum_k [x_k / \epsilon_i(x_k)^2]}. \quad (3)$$

We assume that $x_{k+1} - x_k = \delta x \rightarrow 0$; i.e., the experiment has a fine grid in x . Furthermore, we assume that $\epsilon \rightarrow 0$; i.e., measurements in both experiments enjoy tiny error bars. With these assumptions, we write $a_1 = \int_{x_1}^{x_N} \mathcal{A}(x) x dx / \int_{x_1}^{x_N} x^2 dx$ and $a_2 = \int_{x_1}^{x_N} x \mathcal{A}^{-1}(x) dx / \int_{x_1}^{x_N} [x \mathcal{A}^{-1}(x)]^2 dx$. We see that the first experiment leads to $a_1 \simeq 1.0010$. The second experiment yields $a_2 \simeq 1.0020$ [23]. Even though the two values are very close to each other, they are different. This reflects the fact that the first experiment trusts all points equally [$\epsilon_1(x_1) = \epsilon_1(x_N)$], whereas the second has more confidence in nonuniversal points [e.g., $\epsilon_2(x_1)/\epsilon_2(x_N) \simeq x_1/x_N < 1$]. Note that within the realm of each numerical experiment, the values of a_1 and a_2 are exact as $\epsilon \rightarrow 0$, and they contradict each other. (It is easy to check numerically that $a_1 \neq a_2$ even if we assume that there is some variation in the error bars, e.g., if ϵ is a random number drawn from a normal distribution with the mean $\tilde{\epsilon}$ and the standard deviation $\tilde{\epsilon}/10$.)

The systematic error discussed above is based on two facts. First, the universal model is an underfit model; i.e., it does not describe the data sufficiently well when $\epsilon \rightarrow 0$. Second, we *systematically* force the fitting procedure to trust nonuniversal physics more in the second experiment. One can improve the fitting procedure in this section by introducing other terms, which mimic nonuniversal physics, to the fitting function. Alternatively, if one has some knowledge of the second term in Eq. (1), one can set the upper bound on the error ϵ_i [19] or use the Bayesian parameter estimation [24]. We refrain from utilizing these options here, as (i) there is limited understanding of finite-range effects on three-body recombination at finite temperature and (ii) our aim is to mimic the state-of-the-art analysis of three-body recombination in cold atoms.

The toy model presented in this section is artificial and contains assumptions (e.g., $\epsilon \rightarrow 0$) that might be hard to satisfy experimentally. In spite of this, it illustrates the fact that the parameter a corresponds to a physical quantity only if $x_1 \gg 1$, otherwise a depends on the experimental protocol even for very accurate and dense data sets. To illustrate how the corresponding error might enter the analysis of three-body recombination, we simulate the standard routine for analyzing experiments. To this end, we introduce a finite-range model to generate experimental data. Then we fit these data using the zero-range model of Refs. [25,26].

Model to simulate three-body loss. Typically, a three-boson problem is notoriously difficult to solve. However, in the limit of low energies and short-range interactions one can obtain an accurate solution with a single differential equation for the hyper-radial wave function f in the adiabatic approximation (for review, see Ref. [4])

$$\left(-\frac{d^2}{d\rho^2} + \frac{v^2(\rho) - 1/4}{\rho^2} - \frac{2mE}{\hbar^2} \right) f(\rho) = 0, \quad (4)$$

where E is the energy, m is the mass of a boson, and ρ is the hyper-radius [27]. The function $v(\rho)$ determines the effective three-body potential from two-body interactions. In spite of the simplicity of Eq. (4), it provides a valuable tool in studies of universal properties of three-body states [28,29] and associated with them losses in cold gases (see, e.g., Refs. [30,31]).

For a fixed value of ρ , the parameter ν solves the equation

$$\frac{8}{\sqrt{3}} \sin \frac{\nu\pi}{6} - \nu \cos \frac{\nu\pi}{2} = \sqrt{2}\rho \left(\frac{1}{|a|} + F \right) \sin \frac{\nu\pi}{2}, \quad (5)$$

where a is the scattering length, and F contains information about finite-range corrections. If $F = 0$, then Eq. (5) leads to the “zero-range” model (see, e.g., Refs. [12,25,26]). It describes three-body recombination rates accurately, assuming that the fitting parameters a_- and η might depend on the temperature [11,12]. The aim of this section is to provide an algorithm for generating the experimental data of three-body recombination using a finite-range model with $F \neq 0$ [32].

To investigate finite-range effects, we use the following expression of F [33,34],

$$F(\rho) = \frac{R}{4} \frac{\nu^2}{\rho^2}, \quad (6)$$

where R is a new length scale in the problem—the effective range parameter that appears in two-body scattering. It is worth noting that studies based upon hyperspherical formalism as well as effective field theories suggest the existence of one more three-body parameter once range corrections are considered [35–37]. As our aim here is to design a minimal model for studying systematic errors possible in the experiment, we refrain from introducing this additional parameter. We note that, in the hyperspherical formalism, its effect is canceled (at least partially) by nonadiabatic corrections [35].

In one-channel atom-atom scattering, the parameter R is typically positive (see, e.g., Refs. [38,39]). However, in multichannel problems, which are more suitable for modeling ultracold setups, this parameter is negative [40], and thus, we assume $R < 0$ (see Ref. [41] for a discussion of the case with $R > 0$) [42].

The solution to Eq. (5) as a function of $\rho/|a|$ is plotted in Ref. [41]. The main features of the solutions are as follows. In the zero-range model ($R = 0$), $\nu^2(0) \approx -1$. This leads to a (super)attractive $-1.26/r^2$ potential in Eq. (4), which supports an infinite number of bound states with the ground state of infinite negative energy—the Thomas collapse [43] (for review, see Refs. [4,6,7]). The collapse occurs only for $R = 0$. In a finite-range model ($R < 0$), the solution to Eq. (5) in the limit $\rho \rightarrow 0$ is determined by R ; $\nu^2(0)$ vanishes and the Thomas collapse does not occur. The long-range part is determined mainly by the scattering length (see Ref. [41]).

In general if $\rho \gg \sqrt{|Ra|}$, then ν^2 is given approximately by ν_{ZR}^2 —the solution of Eq. (5) with $F = 0$. (This estimate is obtained by comparing $1/|a|$ and F assuming that ν is of the order of unity.) In this limit we can derive

$$\nu^2 \simeq \nu_{\text{ZR}}^2 + \frac{R}{\rho} g \left(\frac{\rho}{a} \right), \quad (7)$$

where g is given in Ref. [41]. In our numerical simulations, this expansion is accurate already for $\rho \gtrsim 2|R|$. Note that the parameter R enters linearly in this expression. Therefore, positive (negative) values of R lead to larger (smaller) values of the effective potential.

Loss coefficient. At $\rho \rightarrow \infty$, any solution to Eq. (4) for $E > 0$ can be written as a combination of incoming and

TABLE I. Parameters of the zero-range model (a_- and η) and the finite-range model (r and ϕ) for $R = -55a_0$ from fitting to the experimental data of Ref. [12]. The last row presents the average values. The shown values of χ^2 are normalized by the number of data points.

T (nK)	$ a_- $	η	χ_0^2	r	ϕ	χ^2
178	772	0.24	0.5	1.7	2.2	0.4
192	718	0.22	0.5	1.3	2.1	0.4
286	824	0.25	0.2	2.1	2.2	0.1
304	769	0.31	0.4	1.9	2.0	0.3
Avg.	771	0.26		1.8	2.1	

outgoing waves:

$$f(\rho \rightarrow \infty) \rightarrow H e^{-i\sqrt{2}k\rho} + G e^{i\sqrt{2}k\rho}, \quad (8)$$

where $k = \sqrt{mE/\hbar^2}$. It is intuitively clear that information about losses must be contained in the ratio $|G/H|$. The WKB method of hidden crossing theory can be used to confirm this [9,31,45]. Within this theory, the recombination coefficient for a given value of k is written as

$$\alpha_k(k) = 36(2\pi)^2 \sqrt{3} \frac{\hbar}{mk^4} \left(1 - \left| \frac{G}{H} \right|^2 \right). \quad (9)$$

We show in Ref. [41] that the ratio G/H depends on a complex parameter A that defines short-range three-body physics (not fixed by the effective range) via

$$f(\rho \rightarrow 0) \sim \sqrt{k\rho} [A + \ln(\rho/|R|)]. \quad (10)$$

This parameter is determined by fitting to the experimental data; see Table I for typical values of r and ϕ ($A = r e^{i\phi}$).

The recombination coefficient for a fixed temperature can now be obtained by thermally averaging with the Boltzmann

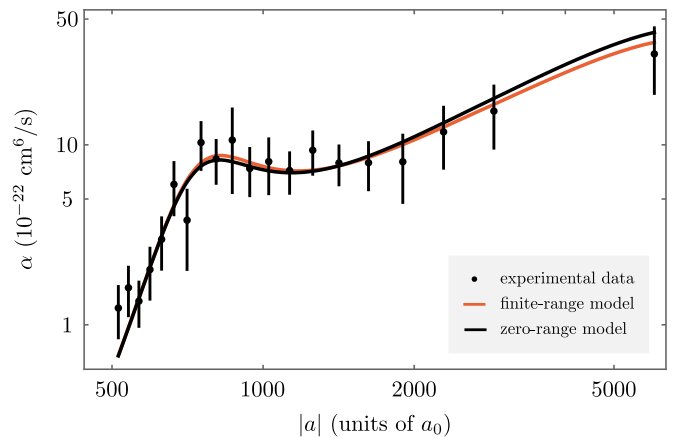


FIG. 2. Recombination coefficient α from the experiment of Ref. [12] at $T = 178$ nK (dots with error bars). The figure also shows the fit to the zero-range model (black) and to the finite-range model (orange) with $R = -55a_0$ (a_0 is the Bohr radius). The value of $|R|$ is chosen close to the corresponding van der Waals length $R_{\text{vdW}} = 64.53a_0$ [44].

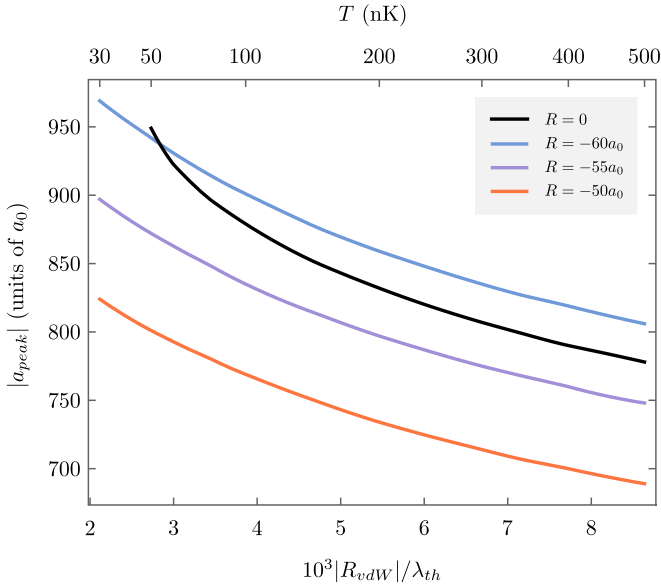


FIG. 3. Peak of recombination, $|a_{\text{peak}}|$, as a function of temperature for different values of the effective range. $\lambda_{\text{th}} = \hbar/\sqrt{2\pi m k_B T}$ (cf. Ref. [11]), so $10^3 |R_{\text{vdW}}|/\lambda_{\text{th}} \propto \sqrt{T}$. Parameters of the finite-range model are as follows: $r = 1.8$ and $\phi = 2.1$; the zero-range model has $|a_-| = 771a_0$ and $\eta = 0.26$ (cf. Table I).

distribution [9,46]:

$$\alpha = \frac{1}{2(k_B T)^3} \int \alpha_k E^2 e^{-E/k_B T} dE. \quad (11)$$

Here, we have assumed that a Bose gas forms a thermal cloud and that it is so dilute that many-body effects can be neglected. α from Eq. (11) fits well the experimental data. We illustrate this in Fig. 2 using the data from Ref. [12]. The figure shows the fit based upon the finite-range model from Eq. (11) together with the zero-range model (obtained with $R = 0$, see also Refs. [12,26]). Both fits describe the data equally well; i.e., they lead to similar values of χ^2 (see Table I).

Equation (11) will be used in this work only to simulate “experimental” data, which are “realistic” in the sense that they contain beyond-zero-range effects. However, note that the finite-range model can be used to understand beyond-zero-range physics in the context of finite-temperature effects. To motivate further analysis of the model, we present the temperature dependence of the recombination peak location $|a_{\text{peak}}|$ extracted from Eq. (11) (see Fig. 3). $|a_{\text{peak}}|$ increases for smaller temperatures, in agreement with previous studies (see, e.g., Ref. [15]). This behavior is affected by the value of R . We observe that $|a_{\text{peak}}|(R_1) - |a_{\text{peak}}|(R_2) \sim 10(R_1 - R_2)$ for the considered parameters. In-depth investigation of this scaling, which resembles the van der Waals universality, is left for future studies.

Fitting the finite-range model. Using the finite-range model, we generate experimental data for ^{39}K (see a sketch in Fig. 4). As for the toy model, we consider here two experiments that measure $\{\{\alpha_i(a_1), \epsilon_i(a_1)\}, \dots, \{\alpha_i(a_N), \epsilon_i(a_N)\}\}$ at different temperatures; $i = 1$ ($i = 2$) is for the first (second) experiment. For each T and a , we draw values of α_i from a normal distribution whose mean is given by Eq. (11) with $r = 1.8$

and $\phi = 2.1$ (motivated by Table I). The standard deviation is given by $\epsilon_i/2$, which implies that the experimental ($2\text{-}\sigma$) error bar is ϵ_i . We assume that the two experiments measure identical values of the scattering length (chosen in agreement with experimental points of Ref. [12]), which can be determined exactly. The difference between the experiments is only in the values of ϵ_i . Similarly to the toy model, we work with $\epsilon_1(a)$, which is independent of a , and $\epsilon_2(a)$, which is proportional to $\alpha(a)$.

We use $\epsilon_1(a) = 10^{-23} \text{cm}^6/\text{s}$ and $\epsilon_2(a) = \alpha(a)/20$. This implies that all points are equally trustworthy in the first experiment, and the second experiment has the strongest confidence in the measurements in the nonuniversal region.

The resulting data are fitted using the zero-range model [12,25,26] with the standard parametrization a_- and η . The former parameter is shown in Fig. 5 as a function of temperature for different values of the effective range R .

Figure 5 shows that the extracted value of a_- strongly depends on the experimental conditions [47]. For the constant-error experiment, there is a linear dependence of a_- on \sqrt{T} which agrees with Refs. [11,12], although with a different slope. The linear dependence is also seen in the direct fitting of the finite-range model with the zero-range model (without generation of experimental data). In the proportional-error experiment, we observe that a_- is almost temperature-independent in agreement with Ref. [15]. These results suggest that the difference between experimental observations of Ref. [15] and Refs. [11,12] might be explained by the difference in the experimental setups. Admittedly, other explanations cannot be ruled out at the moment. The experiments of Refs. [11,15] might reach different conclusions because they focus on different systems (Cs vs K) and Feshbach resonances. The density of the K cloud in Ref. [12] was probably too high at low temperatures so that many-body effects could have played a role (see also a discussion in Ref. [15]).

In any case, the existing experimental data should be reanalyzed in light of our results. Indeed, the extraction of a_- at $T = 0$ from the data sets in Fig. 5 leads to conflicting results implying that one needs additional information for identifying the “correct” universal value. The difference between the extracted values of $a_-(T = 0)$ in the present example can be more than 5%, which is similar to the accuracy of the state-of-the-art values [15] and, thus, can be decisive in determining the error bars. This estimate suggests the following rule of thumb: a systematic error due to fitting with the zero-range model is of the order of $|R/a_-|$ (cf. Ref. [25]).

Finally, we note that the sign of the slope of $a_-(T)$ in the first experiment (see Fig. 5) is determined by the sign of R (see Ref. [41]). This can be anticipated from the fact that the contribution of R to the hyperspherical potential has a linear in R term, which is perturbative [see Eq. (7)].

Summary and outlook. We argued that the temperature dependence of three-body parameters may reflect certain characteristics of the experiment, and not the underlying three-body physics. In particular, it may reflect our confidence in the accuracy of different data points.

We first considered a toy model in which the universal parameter (the slope of a line at $x \rightarrow \infty$) cannot be extracted reliably by considering only a finite range of x , no matter how many data points are produced by the experiment and how

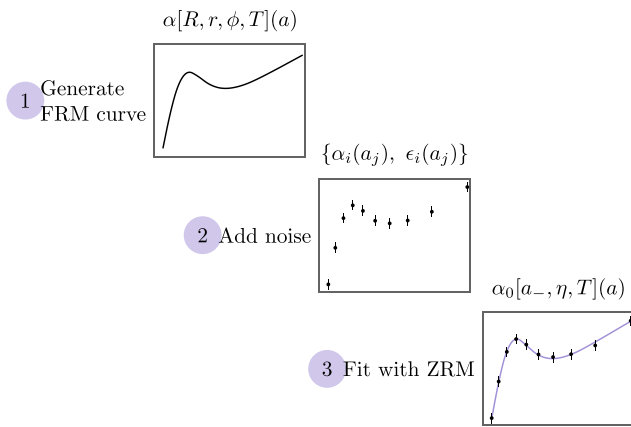


FIG. 4. Generation and analysis of experimental data. First, the recombination coefficient is calculated using the finite-range model (FRM). Second, this curve is used to generate experimental data points from a normal random distribution. The standard deviation is given by $\epsilon_i/2$, which was predetermined by us. Third, the resulting artificial experimental data are fitted using the zero-range model (ZRM), which yields the parameter a_- .

accurate they are. Most importantly, different distributions of error bars in the two considered experiments lead to different fitting parameters; i.e., the conclusions of these experiments are conflicting.

Then, we developed a finite-range model of three-body recombination and showed its good performance in describing experimental data. We used this model to simulate an experiment for a user of an (incomplete) zero-range model. As for the toy model, we showed that the type of error bars can change the value of the extracted fitting parameter a_- by a few percent. This leads to a systematic error in the value of the universal three-body parameters.

Our results might help to reconcile experimental observations of the dependence of a_- on T [11,12,15]. They may

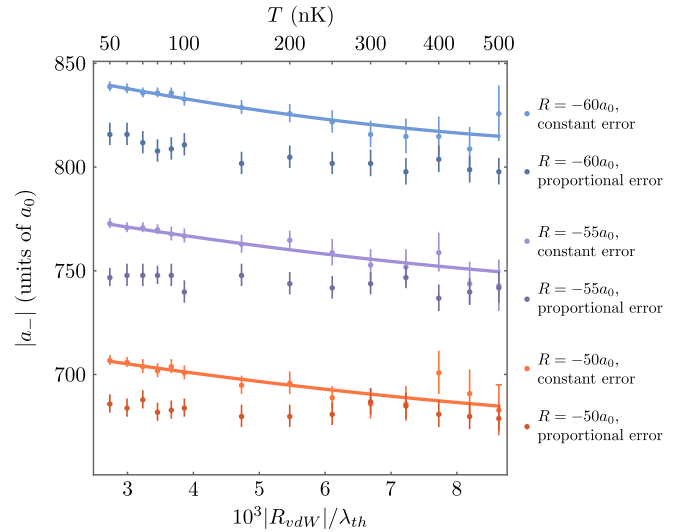


FIG. 5. The three-body parameter a_- obtained from the artificial experimental data generated using the finite-range model with fixed parameters (see Fig. 4). Finite-range model parameters: $r = 1.8$ and $\phi = 2.1$. Solid lines correspond to a direct zero-range model fit of the finite-range model (no added noise and error bars).

also motivate researchers to find approaches for extracting universal parameters from cold-atom data contaminated by nonuniversal physics. For three-body loss, the safest way is to provide measurements at larger scattering length. However, it is demanding from the experimental point of view. Alternatively, one can focus on available “true” observables, such as the peak position of losses. To incorporate information about the finite-range bias, one can assign different weights to the points with the smallest values of $|a|$ [48]. Finally, one can use theoretical finite-range models (such as the one presented above) to model experiments using standard Monte Carlo techniques [49] and subsequently estimate possible systematic error bars.

Acknowledgments. We thank Jan Arlt, Hans-Werner Hammer, and Karsten Riisager for useful discussions. M.L. acknowledges support by the European Research Council (ERC) under Starting Grant No. 801770 (ANGULON).

[1] V. Efimov, Energy levels arising from resonant two-body forces in a three-body system, *Phys. Lett. B* **33**, 563 (1970).
 [2] V. Efimov, Weakly bound states of three resonantly interacting particles, *Sov. J. Nucl. Phys.* **12**, 589 (1971).
 [3] A. Jensen, Special issue on Efimov physics, *Few-Body Syst.* **51**, 77 (2011).
 [4] E. Nielsen, D. Fedorov, A. Jensen, and E. Garrido, The three-body problem with short-range interactions, *Phys. Rep.* **347**, 373 (2001).
 [5] A. S. Jensen, K. Riisager, D. V. Fedorov, and E. Garrido, Structure and reactions of quantum halos, *Rev. Mod. Phys.* **76**, 215 (2004).
 [6] E. Braaten and H.-W. Hammer, Universality in few-body systems with large scattering length, *Phys. Rep.* **428**, 259 (2006).

[7] P. Naidon and S. Endo, Efimov physics: a review, *Rep. Prog. Phys.* **80**, 056001 (2017).
 [8] C. H. Greene, P. Giannakeas, and J. Pérez-Ríos, Universal few-body physics and cluster formation, *Rev. Mod. Phys.* **89**, 035006 (2017).
 [9] J. P. D’Incao, Few-body physics in resonantly interacting ultracold quantum gases, *J. Phys. B: At., Mol. Opt. Phys.* **51**, 043001 (2018).
 [10] R. Grimm, Efimov states in an ultracold gas: How it happened in the laboratory, *Few-Body Syst.* **60**, 23 (2019).
 [11] B. Huang, L. A. Sidorenkov, and R. Grimm, Finite-temperature effects on a triatomic Efimov resonance in ultracold cesium, *Phys. Rev. A* **91**, 063622 (2015).
 [12] L. J. Wacker, N. B. Jørgensen, K. T. Skalmstang, M. G. Skou, A. G. Volosniev, and J. J. Arlt, Temperature dependence

- of an Efimov resonance in ^{39}K , *Phys. Rev. A* **98**, 052706 (2018).
- [13] R. Pires, J. Ulmanis, S. Häfner, M. Repp, A. Arias, E. D. Kuhnle, and M. Weidemüller, Observation of Efimov Resonances in a Mixture with Extreme Mass Imbalance, *Phys. Rev. Lett.* **112**, 250404 (2014).
- [14] C. Chin, R. Grimm, P. Julienne, and E. Tiesinga, Feshbach resonances in ultracold gases, *Rev. Mod. Phys.* **82**, 1225 (2010).
- [15] R. Chapurin, X. Xie, M. J. Van de Graaff, J. S. Popowski, J. P. D’Incao, P. S. Julienne, J. Ye, and E. A. Cornell, Precision Test of the Limits to Universality in Few-Body Physics, *Phys. Rev. Lett.* **123**, 233402 (2019).
- [16] T. Weber, J. Herbig, M. Mark, H.-C. Nägerl, and R. Grimm, Three-Body Recombination at Large Scattering Lengths in an Ultracold Atomic Gas, *Phys. Rev. Lett.* **91**, 123201 (2003).
- [17] The value of a_- is (nearly) universal for many (although not all [15]) alkali atoms—it is determined by the van der Waals length [7–9,50–53].
- [18] R. J. Furnstahl, D. R. Phillips, and S. Wesolowski, A recipe for EFT uncertainty quantification in nuclear physics, *J. Phys. G: Nucl. Part. Phys.* **42**, 034028 (2015).
- [19] B. D. Carlsson, A. Ekström, C. Forssén, D. F. Strömberg, G. R. Jansen, O. Lilja, M. Lindby, B. A. Mattsson, and K. A. Wendt, Uncertainty Analysis and Order-by-Order Optimization of Chiral Nuclear Interactions, *Phys. Rev. X* **6**, 011019 (2016).
- [20] We have checked that one can use other simple expressions, for example, $a_i x + b_i$, without changing the conclusion.
- [21] W. H. Press, S. A. Teukolsky, W. T. Vetterling, and B. P. Flannery, *Numerical Recipes C*, 2nd ed. (Cambridge University, Cambridge, England, 1992).
- [22] P. Young, *Everything you Wanted to Know About Data Analysis and Fitting but Were Afraid to Ask* (Springer International Publishing, 2015).
- [23] $a_i > 1$ because $\mathcal{A}(x)/x > 1$ [see Eq. (1)].
- [24] S. Wesolowski, N. Klco, R. J. Furnstahl, D. R. Phillips, and A. Thapaliya, Bayesian parameter estimation for effective field theories, *J. Phys. G: Nucl. Part. Phys.* **43**, 074001 (2016).
- [25] E. Braaten, H.-W. Hammer, D. Kang, and L. Platter, Three-body recombination of identical bosons with a large positive scattering length at nonzero temperature, *Phys. Rev. A* **78**, 043605 (2008).
- [26] B. S. Rem, A. T. Grier, I. Ferrier-Barbut, U. Eismann, T. Langen, N. Navon, L. Khaykovich, F. Werner, D. S. Petrov, F. Chevy, and C. Salomon, Lifetime of the Bose Gas with Resonant Interactions, *Phys. Rev. Lett.* **110**, 163202 (2013).
- [27] $\rho = \sqrt{2/3} \sqrt{r_1^2 + r_2^2 + r_3^2 - \mathbf{r}_1 \cdot \mathbf{r}_2 - \mathbf{r}_2 \cdot \mathbf{r}_3 - \mathbf{r}_1 \cdot \mathbf{r}_3}$, where \mathbf{r}_i is the coordinate of the i th particle.
- [28] D. V. Fedorov and A. S. Jensen, Efimov effect in coordinate space Faddeev equations, *Phys. Rev. Lett.* **71**, 4103 (1993).
- [29] E. Nielsen, D. V. Fedorov, and A. S. Jensen, The structure of the atomic helium trimers: halos and Efimov states, *J. Phys. B: At., Mol. Opt. Phys.* **31**, 4085 (1998).
- [30] S. Jonsell, Efimov states for systems with negative scattering lengths, *Europhys. Lett.* **76**, 8 (2006).
- [31] P. K. Sørensen, D. V. Fedorov, A. S. Jensen, and N. T. Zinner, Three-body recombination at finite energy within an optical model, *Phys. Rev. A* **88**, 042518 (2013).
- [32] It might be more appropriate to refer to “the finite-range model” as an “extended zero-range model.” For simplicity, we do not do it here.
- [33] D. V. Fedorov and A. S. Jensen, Regularization of a three-body problem with zero-range potentials, *J. Phys. A: Math. Gen.* **34**, 6003 (2001).
- [34] L. Platter, C. Ji, and D. R. Phillips, Range corrections to three-body observables near a Feshbach resonance, *Phys. Rev. A* **79**, 022702 (2009).
- [35] M. Thøgersen, D. V. Fedorov, A. S. Jensen, B. D. Esry, and Y. Wang, Conditions for Efimov physics for finite-range potentials, *Phys. Rev. A* **80**, 013608 (2009).
- [36] C. Ji, D. R. Phillips, and L. Platter, Beyond universality in three-body recombination: An effective field theory treatment, *Europhys. Lett.* **92**, 13003 (2010).
- [37] C. Ji, D. R. Phillips, and L. Platter, The three-boson system at next-to-leading order in an effective field theory for systems with a large scattering length, *Ann. Phys.* **327**, 1803 (2012).
- [38] B. Gao, Quantum-defect theory of atomic collisions and molecular vibration spectra, *Phys. Rev. A* **58**, 4222 (1998).
- [39] V. V. Flambaum, G. F. Gribakin, and C. Harabati, Analytical calculation of cold-atom scattering, *Phys. Rev. A* **59**, 1998 (1999).
- [40] G. M. Bruun, A. D. Jackson, and E. E. Kolomeitsev, Multi-channel scattering and Feshbach resonances: Effective theory, phenomenology, and many-body effects, *Phys. Rev. A* **71**, 052713 (2005).
- [41] See Supplemental Material at <http://link.aps.org/supplemental/10.1103/PhysRevA.107.L061304> for the asymptotic behavior of three-body potential, technical details of finite-range model and some results for $R > 0$ and it includes Ref. [54].
- [42] Note that in cold-atom experiments, the parameter R can also depend on the external magnetic field, and hence the scattering length [55] For simplicity, we do not consider this dependence here. This assumption is reasonable when the background scattering length is much smaller than the scattering length engineered in the experiment.
- [43] L. H. Thomas, The interaction between a neutron and a proton and the structure of H^3 , *Phys. Rev.* **47**, 903 (1935).
- [44] J. Jiang, J. Mitroy, Y. Cheng, and M. Bromley, Effective oscillator strength distributions of spherically symmetric atoms for calculating polarizabilities and long-range atom-atom interactions, *At. Data Nucl. Data Tables* **101**, 158 (2015).
- [45] E. Nielsen and J. H. Macek, Low-Energy Recombination of Identical Bosons by Three-Body Collisions, *Phys. Rev. Lett.* **83**, 1566 (1999).
- [46] J. P. D’Incao, H. Suno, and B. D. Esry, Limits on Universality in Ultracold Three-Boson Recombination, *Phys. Rev. Lett.* **93**, 123201 (2004).
- [47] Note that the change in the value of a_- is similar to that of a_{peak} : $|a_-(R_1)| - |a_-(R_2)| \sim 10(R_1 - R_2)$.
- [48] The simplest way to implement the latter suggestion is to exclude a few points from the most nonuniversal region (e.g., around x_0 in the toy model) and evaluate the effect of this on the extracted parameter. One must be careful when doing this in the analysis of three-body recombination as there should be enough points smaller than a_- to ensure an accurate result.

- [49] J. E. Gentle, *Random Number Generation and Monte Carlo Methods* (Springer, New York, 2006).
- [50] M. Berninger, A. Zenesini, B. Huang, W. Harm, H.-C. Nägerl, F. Ferlaino, R. Grimm, P. S. Julienne, and J. M. Hutson, Universality of the Three-Body Parameter for Efimov States in Ultracold Cesium, *Phys. Rev. Lett.* **107**, 120401 (2011).
- [51] J. Wang, J. P. D’Incao, B. D. Esry, and C. H. Greene, Origin of the Three-Body Parameter Universality in Efimov Physics, *Phys. Rev. Lett.* **108**, 263001 (2012).
- [52] R. Schmidt, S. Rath, and W. Zwerger, Efimov physics beyond universality, *Eur. Phys. J. B* **85**, 386 (2012).
- [53] P. Naidon, S. Endo, and M. Ueda, Physical origin of the universal three-body parameter in atomic Efimov physics, *Phys. Rev. A* **90**, 022106 (2014).
- [54] H.-W. Hammer, T. A. Lähde, and L. Platter, Effective-range corrections to three-body recombination for atoms with large scattering length, *Phys. Rev. A* **75**, 032715 (2007).
- [55] P. K. Sørensen, D. V. Fedorov, A. S. Jensen, and N. T. Zinner, Finite-range effects in energies and recombination rates of three identical bosons, *J. Phys. B: At., Mol. Opt. Phys.* **46**, 075301 (2013).